JGR Oceans

RESEARCH ARTICLE
10.1029/2020JC016147

Observations and a Model of Net Calcification Declines in Palau's Largest Coral Reef Lagoon Between 1992 and 2015

Steven J. Lentz[1], Anne L. Cohen[1], Kathryn E. F. Shamberger[2], and Hannah Barkley[3]

[1]Woods Hole Oceanographic Institution, Woods Hole, MA, USA, [2]Department of Oceanography, Texas A&M University, College Station, TX, USA, [3]Joint Institute for Marine and Atmospheric Research, NOAA Pacific Islands Fisheries Science Center, Honolulu, HI, USA

Key Points:
- Calcification in Palau's largest coral reef lagoon declined 50% due to a loss of coral cover following the 1998 bleaching event
- Palau's largest coral reef lagoon has not recovered from the 1998 bleaching event as of 2015
- Spring-neap tidal variations in residence time cause substantial variations in lagoon alkalinity not related to calcification rates

Correspondence to:
S. J. Lentz,
slentz@whoi.edu

Citation:
Lentz, S. J., Cohen, A. L., Shamberger, K. E. F., & Barkley, H. (2020). Observations and a model of net calcification declines in Palau's largest coral reef lagoon between 1992 and 2015. *Journal of Geophysical Research: Oceans*, *125*, e2020JC016147. https://doi.org/10.1029/2020JC016147

Received 11 FEB 2020
Accepted 23 JUN 2020
Accepted article online 6 JUL 2020

Abstract Net ecosystem calcification (*NEC*) rates of Palau's largest lagoon and barrier reef system between 1992 and 2015 are estimated from sparse total alkalinity (*TA*) and salinity measurements and a tidal exchange model in which surface lagoon water transported offshore on the ebb tide is replaced by saltier (denser) ocean water that sinks to the bottom after entering the lagoon on the flood tide. Observed lagoon salinities are accurately reproduced by the model with no adjustable parameters. To accurately reproduce observed lagoon *TA*, *NEC* for the lagoon-barrier reef system was 70 mmols m^{-2} day^{-1} from 1992 to 1998, 35 mmols m^{-2} day^{-1} from 1999 to 2012, and 25 mmols m^{-2} day^{-1} from 2013 to 2015. This indicates that Palau's largest lagoon and barrier reef system has not recovered, as of 2015, from the 50% decline in *NEC* in 1998 caused by the loss of coral cover following a severe bleaching event. The cause of the further decline in *NEC* in 2012–2013 is unclear. Lagoon residence times vary from 8 days during spring tides to 14 days during neap tides and drive substantial spring-neap variations in lagoon *TA* (~25% of the mean salinity-normalized ocean-lagoon *TA* difference). Sparse measurements that do not resolve these spring-neap variations can exhibit apparent long-term variations in alkalinity that are not due to changes in *NEC*.

Plain Language Summary The primary objective of this study is to determine long-term variations in the rate at which corals and other organisms are building calcium carbonate skeletons that form the reefs in Palau's largest lagoon and barrier reef system in the western Pacific. Determining long-term variations in the rate at which coral reef structures are either growing or shrinking is critical for assessing the impact of climate change, including global warming and ocean acidification, on coral reefs. Measurements spanning 1992 to 2015, combined with a model of the system, indicate that the rate corals and other organisms were building skeletons declined by 50% in 1998 because of a loss of coral cover following a severe coral bleaching event. As of 2015, this coral reef system has not recovered from a devastating bleaching event; in fact, there has been a further decline in the rate corals are building reef structure.

1. Introduction

Coral reefs modify the alkalinity of the sea water passing over them as corals, and other calcifiers remove carbonate ions to build calcium carbonate skeletons and ultimately the reef structure. Consequently, alkalinity observations are a potentially useful, quantitative measure of how reefs are responding to changes in ocean conditions (e.g., Cyronak et al., 2018), particularly ocean warming, ocean acidification, and sea level rise, which are expected to substantially impact coral reefs (e.g., Andersson & Gledhill, 2013; Hughes et al., 2017; Perry et al., 2018). However, few coral reefs have been sampled over multiple years or decades, and for those that have, the observations are generally sparse with only a few sets of alkalinity measurements separated by years or even decades (e.g., Davis et al., 2019; Shamberger et al., 2018; Silverman et al., 2007, 2012, 2014; Watanabe et al., 2006). This makes it difficult to determine whether the observed changes in alkalinity are characteristic of longer term trends associated with climate change or shorter time scale variability associated with other processes (e.g., Davis et al., 2019; Shamberger et al., 2018). Determining the net rate at which a coral reef ecosystem is calcifying or dissolving (net ecosystem calcification, *NEC*) is also challenging because processes other than calcification/dissolution influence alkalinity. Significant changes in alkalinity can also be caused by physical processes including variations in: circulation that determine the

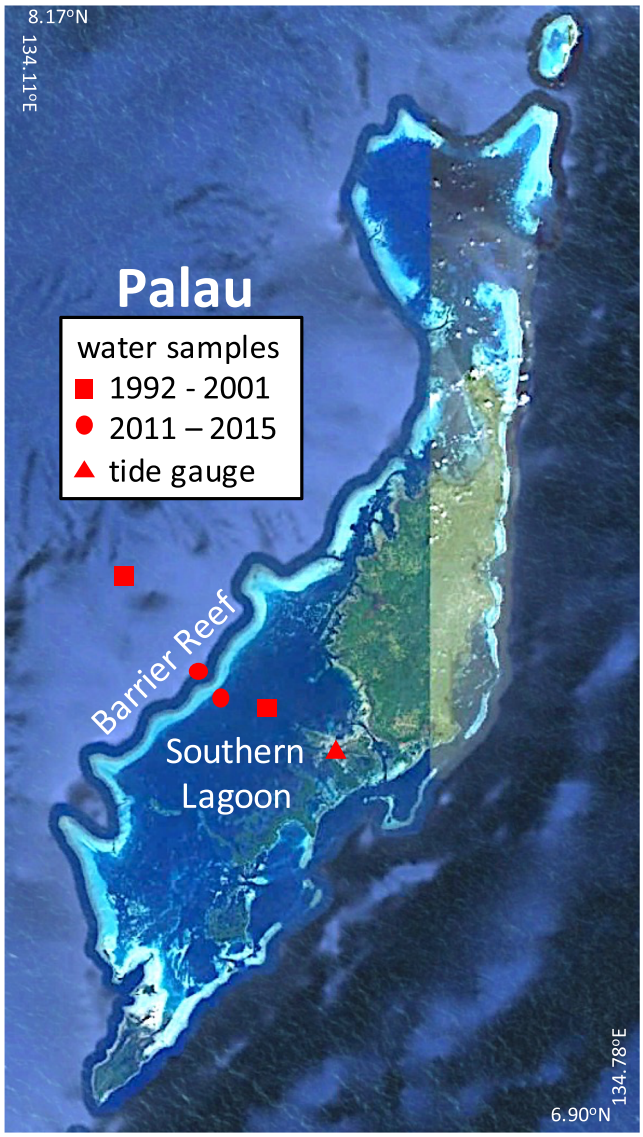

Figure 1. Study region (GoogleEarth) showing approximate sample locations in Palau's Southern Lagoon and adjacent ocean. In September 2011 and August 2014 samples were collected closer to the middle of the lagoon and in August 2014 the ocean sample was farther offshore.

length of time (residence time) a parcel of water spends over a coral reef or in a coral lagoon, sea level or stratification that change the volume of water affected by calcification, source water alkalinity input from the offshore ocean and river runoff, and dilution/concentration by precipitation and evaporation.

Long-term changes in *NEC* of Palau's largest coral reef lagoon (Southern Lagoon) (Figure 1) are determined from total alkalinity (*TA*) measurements made during a sequence of field programs between 1992 and 2015 (Barkley et al., 2015; Kayanne et al., 1993, 2005; Shamberger et al., 2014; Suzuki, 1995; Suzuki & Kawahata, 2003; Watanabe, 2004, 2006). The main island of Palau (Balbeldaob) in the western tropical Pacific is surrounded by an extensive barrier reef that encompasses the large Southern Lagoon (Ngertachebeab) and numerous smaller islands and lagoons. Palau's Southern Lagoon is 40 km long and 12.5 km wide with a surface area of 500 km^2 (Maragos & Cook, 1995; areas and lengths were independently estimated using Google Earth) and an average depth of ~20 m (Watanabe et al., 2006). The lagoon is bounded to the east and north by a nearly continuous set of islands separated by a few narrow channels and to the west and south by an 86 km long barrier reef (Ngerdiluches) (Maragos & Cook, 1995) that is on average 1.5 km wide and 1.5 m deep. The Southern Lagoon contains 683 patch reefs and 491 small islands (Maragos & Cook, 1995).

The carbonate chemistry of the Southern Lagoon and adjacent barrier reef was previously examined by Watanabe et al. (2006) using observations collected between 1992 and 2002. They found that the salinity normalized total alkalinity ($nTA = TA\ S_{ref}/S$ where S is salinity and $S_{ref} = 34$ psu is a reference salinity) in the ocean offshore of the barrier reef was relatively constant (2,220 μmols kg^{-1}), while the Southern Lagoon *nTA* was lower and more variable than the ocean *nTA* (Figure 2). The Southern Lagoon *nTA* increased from 2,136 μmols kg^{-1} in 1992 to 2,175 μmols kg^{-1} in 1999 and then was relatively constant from 1999 to 2002. Watanabe et al. (2006) attributed the increase in the lagoon *nTA* toward oceanic values between 1992 and 1999 to a reduction in *NEC* over the barrier reef and in the lagoon, partially caused by a loss of coral following a severe coral bleaching event in the fall of 1998 (Barkley & Cohen, 2016; Bruno et al., 2001).

Additional water samples were collected in the same region as the previous studies between 2011 and 2015 (Figure 2) as part of studies that provided a broader description of the water chemistry across the Palau archipelago (Barkley et al., 2015; Shamberger et al., 2014). Building on the previous work of Watanabe et al. (2006), the combined data sets spanning 1992 through 2015 are used here to characterize long-term variations in the water chemistry of the Southern Lagoon, determine the cause of the variations, make long-term estimates of *NEC* for the lagoon-barrier reef system, and place focused studies of *NEC* over the barrier reef (Kayanne et al., 2005, Shamberger et al. in prep) in a broader context. While this data set has substantially more observations, 15 sets of average *TA* values spanning 1992 to 2015, than most previous long-term studies (e.g., Davis et al., 2019; Shamberger et al., 2018; Silverman et al., 2012, 2014) there are still only one or two observations (average *TA* over days to a week) per year with an 8 year gap (2003–2010) (Figure 2). Consequently, to aid in the interpretation of this sparse data and to separate signals associated with calcification from other processes, a simple model of the *TA* and salinity variability in the Southern Lagoon driven by tidal exchange between the ocean and the lagoon is developed and validated using the observations (section 2). Two key results of this study are as follows: The long-term *NEC* estimates indicate (1) that the Southern Lagoon-barrier reef system has not recovered from the loss of coral cover caused by the 1998 bleaching event that caused a 50% decline in *NEC* at least

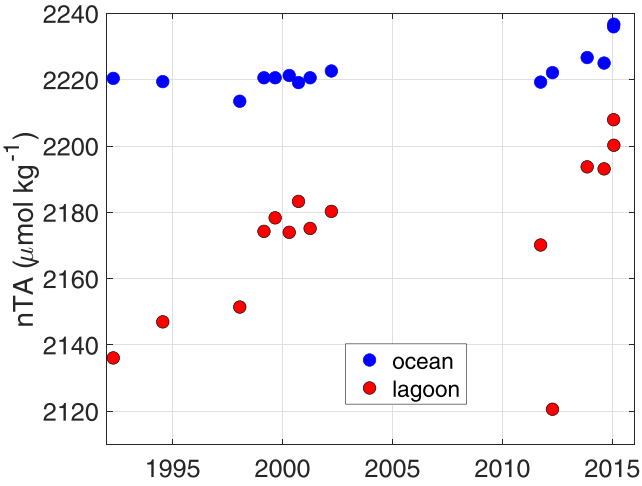

Figure 2. Time series of normalized total alkalinity *nTA* (reference salinity 34 psu) from water samples collected in the ocean offshore of the barrier reef and in the Southern Lagoon (sites Figure 1).

through 2015, and (2) that substantial spring-neap tidal variations in lagoon residence time and, hence *nTA,* that are not resolved by sparse measurements can lead to apparent long-term variations in alkalinity that are not due to changes in *NEC*.

2. Model of Ocean-Lagoon Tidal Exchange

2.1. Conceptual Model

Two physical features provide the basis for a model of the tidal exchange between the ocean and the Southern Lagoon. First, the Southern Lagoon water is typically less salty and hence less dense than the surrounding ocean because precipitation exceeds evaporation and there is significant runoff from the watershed on the northeastern side of the lagoon (Watanabe et al., 2006; see also section 4.3). Second, exchange between the ocean and the Southern Lagoon across the barrier reef is predominately tidal (Figure 3; Kayanne et al., 2005; Lentz et al., 2017; Watanabe et al., 2006). The tidal currents are strong enough that ocean water typically crosses the barrier reef and enters the lagoon each tidal cycle, that is, water parcel displacements over a half tidal cycle range from 1 to 8 km, typically larger than the barrier reef width (1.5 km).

These two physical features control the exchange of salinity and alkalinity between the ocean and the lagoon. As the tide rises (floods), near-surface ocean water flows across the barrier reef and when it enters the lagoon sinks to the bottom because it is saltier and hence denser than the lagoon water (Figure 4). A salinity section across the barrier reef and Southern Lagoon (Figure 4a; from Watanabe et al., 2006) is consistent with this picture as the near-bottom water in the lagoon has the same salinity as the oceanic near-surface waters. As the tide falls (ebbs), near-surface lagoon water is carried offshore across the barrier reef (not shown) and once it reaches the ocean presumably mixes with the ocean water and is advected away from the barrier reef. The latter assumption is supported by the observation that ocean salinity samples near the barrier reef generally track regional ocean salinities (Figure 5b). The tidal exchange across the barrier reef constantly adds oceanic water to the bottom of the lagoon and removes surface water from the lagoon, leading to a gradual upward motion of the water in the lagoon. The tidal range of ~1 m implies 1 m of water over the entire surface area of the lagoon is replaced each tidal cycle. Since the average depth of the lagoon is about 20 m (Watanabe et al., 2006), this suggests that the residence time of the water within the lagoon is ~20 tidal cycles, that is, ~10 days.

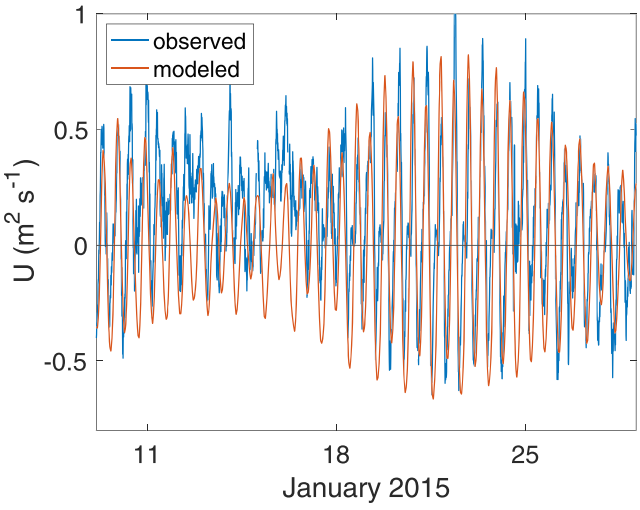

Figure 3. Time series of the measured and modeled (Equation 8) transport across the barrier reef during the January 2015 deployment.

In this conceptual framework, calcification reduces the alkalinity of the lagoon water in two distinct steps. First, as the ocean water crosses the barrier reef, calcification reduces the alkalinity (it typically takes hours for water to cross the barrier reef; Watanabe et al., 2006). In Figure 4b (Watanabe et al., 2006), the *nTA* of the bottom water in the lagoon (2,260 μmols kg^{-1}) is about 30 μmols kg^{-1} lower than the near-surface ocean water, presumably due to calcification over the barrier reef reducing the alkalinity. This is an upper bound on the reduction in *nTA* due to barrier reef calcification because mixing with the ambient lagoon water would further reduce the *nTA* of the water reaching the bottom of the lagoon. Second, over the ~10 day residence time of the lagoon, *nTA* continues to decrease due to calcification within the lagoon. This accounts for the gradual decrease in *nTA* from 2,260 μmols kg^{-1} at the bottom of the lagoon to 2,240 μmols kg^{-1} near the surface seen in Figure 4b. Near-surface lagoon water that passes over the barrier reef but then returns to the lagoon, that is, does not exit to the ocean, may also contribute to the lower near-surface *TA* within the lagoon (section 4.3).

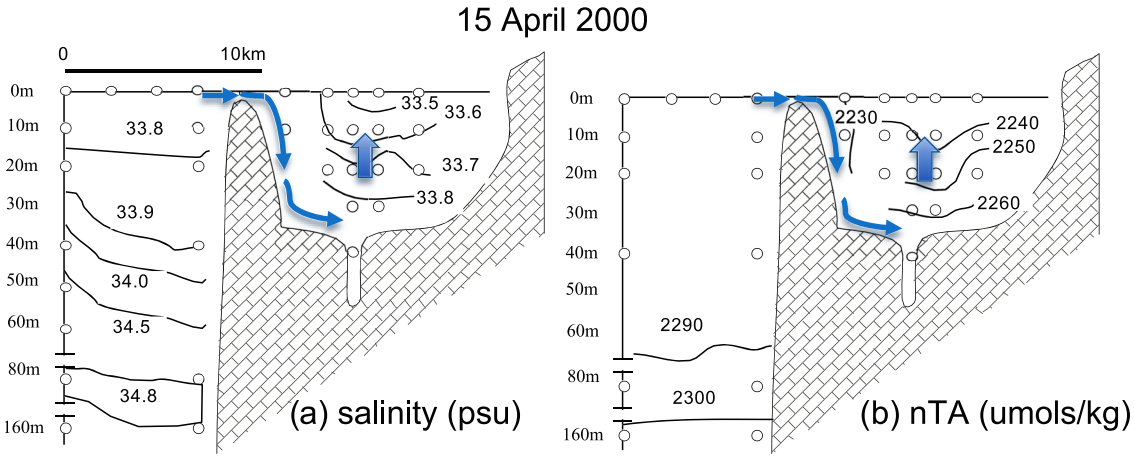

Figure 4. Ocean-lagoon (a) salinity and (b) *nTA* sections from Watanabe et al. (2006) (who used a reference salinity of 35 psu). Blue arrows indicate ocean water path during flood tide. Lighter arrow indicates gradual upward motion of lagoon water over about 20 tidal cycles (10 days).

2.2. Quantitative Model Description

A quantitative model of the salinity and *TA* variability in the Southern Lagoon is formulated based on the conceptual model of tidal exchange in section 2.1 and volume, salt, and *TA* budgets for the lagoon. The key elements of the model are summarized here and a detailed derivation is given in the Appendix. Consideration of the volume budget for the lagoon indicates that the net volume of ocean water transported into the lagoon is

$$Q_F = A_L\Delta\eta_F - A_R h_S - [A_L(P-E)+R]\Delta t/2 \quad (1)$$

and the net volume of lagoon water transported out of the lagoon is

$$Q_E = A_L\Delta\eta_E + A_R h_S - [A_L(P-E)+R]\Delta t/2 \quad (2)$$

In Equations 1 and 2 $A_L = 500$ km^2 is the surface area of the lagoon, $\Delta\eta_F$ (positive) and $\Delta\eta_E$ (negative) are the spatially average sea level changes in the lagoon over the flood and ebb tides, $A_R = 125$ km^2 is the surface area of the barrier reef, h_S is the water depth over the barrier reef at the start of the flood tide, P and E are the precipitation and evaporation rates over the lagoon, R is the river runoff into the lagoon, and Δt is the duration of a tidal cycle (~12.42 hr). Equation 1 states that the volume of ocean water entering the lagoon (transport into the lagoon is positive) is the total volume of water entering the lagoon on the flood tide ($A_L\Delta\eta_F$) minus the volume of lagoon water left over the barrier reef at the start of the flood tide ($A_R h_S$) and minus the net freshwater flux (precipitation, evaporation, and runoff) into the lagoon during the flood tide (half a tidal cycle). Equation 2 states that the total volume of lagoon water leaving the lagoon is the volume of water leaving the lagoon on the ebb tide ($A_L\Delta\eta_F$) (transport out of the lagoon is negative), plus the volume of lagoon water entering the lagoon from the barrier reef at the start of the flood tide ($A_R h_S$) and minus the net freshwater flux. Note that in contrast to the flood tide, only lagoon water is transported offshore on the ebb tide because the ocean water entering the lagoon sinks below the surface layer.

The change in the volume averaged lagoon salinity over each tidal cycle, ΔS_L^A, based on the lagoon salt budget and the volume budget is (Appendix)

$$\Delta S_L^A = \left(\frac{\Delta\eta_F}{h_L} - \frac{A_R h_S}{A_L h_L}\right)\left(S_O - S_L^A\right) - \left[\frac{(P-E)}{h_L} + \frac{R}{A_L h_L}\right]\Delta t\frac{\left(S_O + S_L^A\right)}{2} \quad (3)$$

where $h_L = 20$ m is the average depth of the lagoon and for simplicity we assume the lagoon is well mixed following Watanabe et al. (2006). Equation 3 states that the change in the average lagoon salinity over a tidal cycle ΔS_L^A is due to the net transport of near-surface ocean salinity S_O into the lagoon during the flood tide minus the net transport of near-surface lagoon salinity S_L^S out of the lagoon during the ebb tide and a reduction of the lagoon salinity due to the net fresh water volume flux over the tidal cycle.

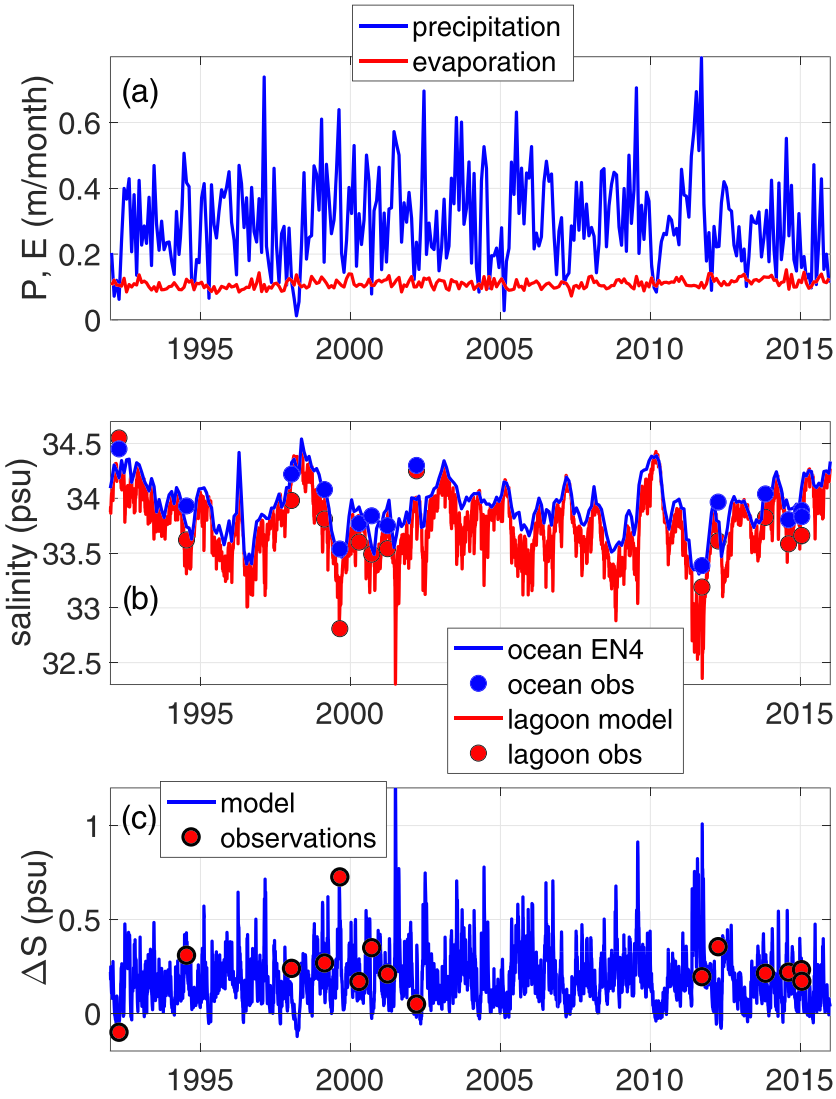

Figure 5. Time series of (a) monthly precipitation and evaporation, modeled and observed (b) ocean and lagoon salinities, and (c) ocean minus lagoon salinities.

The corresponding change in the volume average total alkalinity of the lagoon over each tidal cycle, ΔTA_L^A, is

$$\Delta TA_L^A = \left(\frac{\Delta\eta_F}{h_L} - \frac{A_R}{A_L}\frac{h_S}{h_L}\right)\left(TA_O - TA_L^A\right) - \frac{(P-E)}{h_L}\Delta t\frac{\left(TA_O + TA_L^A\right)}{2} - \frac{R}{A_L h_L}\Delta t\left(\frac{\left(TA_O + TA_L^A\right)}{2} - TA_{river}\right) - \frac{2NEC_B}{\rho h_L}\Delta t \quad (4)$$

In Equation 4, TA_O is the near-surface ocean alkalinity, $TA_{river} = 300$ μmols kg^{-1} is the alkalinity of the river runoff (Watanabe et al., 2006), and $\rho = 1021$ kg/m^3 is the density of sea water and again the lagoon is assumed to be well mixed. NEC_B is a bulk net ecosystem calcification rate for the combined lagoon and barrier reef system given by (Appendix)

$$NEC_B = NEC_L + NEC_R\frac{A_R}{(A_L + A_R/2)}\left(1 - \frac{A_R}{A_L}\frac{h_S}{\Delta\eta_F}\right) \quad (5)$$

where NEC_L and NEC_R are the net ecosystem calcification rates for the lagoon and barrier reef, respectively. The TA budget differs from the salinity budget primarily in the additional term accounting for calcification (NEC) over the barrier reef and in the lagoon.

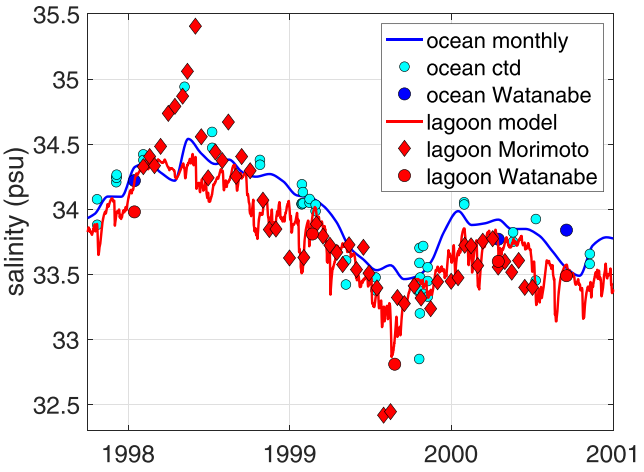

Figure 6. Time series of ocean (blue) and lagoon (red) salinities from late 1997 to 2000. Lines are ocean salinity from EN4 monthly climatology (blue) and resulting model estimate of the lagoon salinity (red). Symbols are observed salinities including regional measurements from EN4 database (cyan ocean ctd).

This quantitative model is conceptually similar to the two residence time estimates for the lagoon made by Watanabe et al. (2006). The primary difference is that the model proposed here provides an explicit formulation for tidal exchange rather than estimating a single representative residence time (see section 3.1). Watanabe et al. (2006) made two estimates of the residence time. The first residence time estimate is based on the tidal range and water depth as described in section 2.1 but assuming an exponential decay. The second residence time estimate is inferred from a simplified version of the salt budget (Equation 3). In this study, comparison of the observed and model lagoon salinities provides an independent evaluation of the tidal exchange model that is particularly useful because there are no adjustable parameters in the model estimates of the lagoon salinity (Equation 3).

2.3. Model Implementation, Inputs, and Validation Data

Time series of the lagoon salinity and *TA* are estimated by stepping Equations 3 and 4 forward in time each tidal cycle given time series of the change in sea level over each flood tide $\Delta\eta_F$, the ocean inputs S_O and TA_O, precipitation P and evaporation E rates, and an inferred NEC_B. River runoff is estimated as $R = A_{WS}P$, where $A_{WS} = 200$ km^2 is the area of the water shed (Watanabe et al., 2006) and evaporation of the runoff is accounted for following Watanabe et al. (2006). The initial lagoon salinity and *TA* are set to ocean values at the beginning of 1991. This allows a year for the system to equilibrate, which is much longer than the lagoon adjustment time scale of 8–14 days (section 3.1).

The change in sea level over each flood tide $\Delta\eta_F$ and the water depth over the barrier reef at the start of each flood tide h_S are estimated from hourly sea level observations from the Malakal tide gauge (Figure 1, triangle), obtained from the University of Hawaii Sea Level Center (Caldwell et al., 2015). Comparisons of the tide gauge measurements with pressure measurements at the seaward and lagoon edges of the barrier reef and an inner lagoon indicate that spatial variations in sea level within the Palau reef-lagoon system are small (standard deviations 1–3 cm) relative to the tidal range (~1 m).

Daily precipitation rates from the Koror airport meteorological station were obtained from National Climate Data Center's Global Historical Climate Network and daily evaporation rates for the region around Palau from the Woods Hole Oceanographic Institution's Objectively Analyzed air-sea Fluxes climatology (http://oaflux.whoi.edu). Objectively mapped monthly near-surface ocean salinity and temperatures and the corresponding individual CTD measurements for the region (Figures 5b and 6) were obtained from the Met Office Hadley Centre EN4.2.1 hydrographic database (Good et al., 2013). Ocean *TA* was estimated using the monthly near-surface ocean salinities and the empirical relationship

$$TA_O = 2285 + 64.2(S_O - 35) \quad (6)$$

derived from the ocean salinity and *TA* measurements (Figures 5b and 7a, blue circles). Equation 6 is similar to empirical salinity *TA* relationships from open ocean observations from the equatorial Pacific (e.g., Lee et al., 2006). The primary difference is the constant term in Equation 6 ($TA_O = 2285$ μmols kg^{-1} at $S_O = 35$ psu) is about 10 μmols kg^{-1} less than for the open ocean estimates in the region (discussed in section 4.1). Daily precipitation and evaporation, and monthly ocean salinity was interpolated to tidal times (~12.5 hr).

The salinity and *TA* measurements made between 1992 and 2002 were from the center of the Southern Lagoon and in the ocean ~10 km offshore of the barrier reef (Figure 1; Watanabe et al., 2006). The relevant observations from the 2011–2015 studies focused on the barrier reef, so ocean and lagoon measurements were made within a few hundred meters of the barrier reef, except for lagoon samples in 2011 and the lagoon and ocean samples in 2014. Ocean samples taken during ebb tide that might contain lagoon water and lagoon samples taken during flood tide that might contain ocean water were excluded from the analyses. Fifty-three lagoon salinity samples collected near the Malakal tide gauge (Figure 1) from 1998 to 2000 (Morimoto et al., 2002) are also compared to the model salinities.

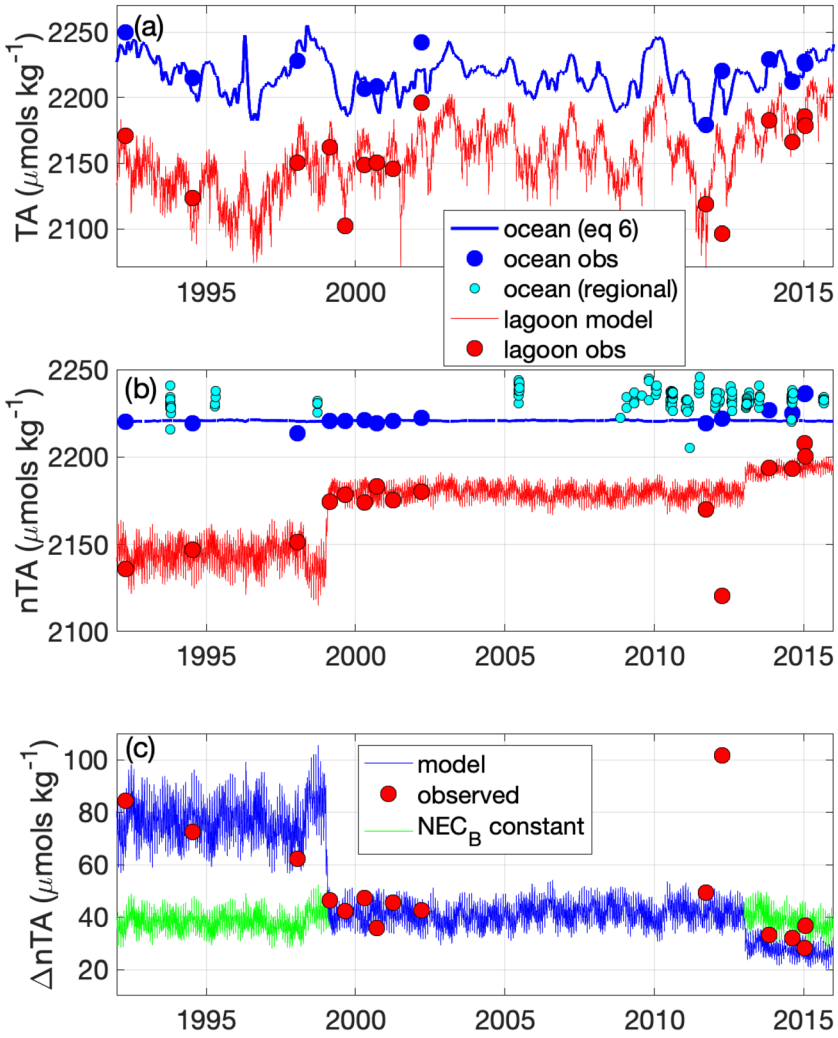

Figure 7. Time series of (a) *TA* ocean (blue) and lagoon (red), (b) *nTA* (reference salinity 34 psu), and (c) Δ*nTA* the difference between the ocean and lagoon. Symbols are observations. Blue lines in (a) and (b) are ocean *TA* and *nTA* estimates from (6). Red line in (b) and blue line in (c) are model estimates using three step $NEC_B = 70$ mmols m^{-2} day^{-1} before 1998, 35 mmols m^{-2} day^{-1} from 1999–2012, and 25 mmols m^{-2} day^{-1} from 2013–2015. The green line in (c) is model estimate for a constant $NEC_B = 35$ mmols m^{-2} day^{-1}. In b) ocean regional *nTA* from the Global Data Analysis Project data set for the upper 20 m in the region from 0° to 15°N and 120° to 150°E (Olsen et al., 2016) are shown.

A key assumption in comparing the observations and model is that salinity and *TA* measurements at specific locations in the lagoon are representative of the spatially averaged lagoon salinity and *TA*. Across and along lagoon *TA* and salinity sections by Watanabe et al. (2006) provide some support for this assumption. However, as discussed in section 4.3, this assumption may be problematic during certain conditions.

The final model input needed is a time series of NEC_B. The simplest NEC_B time series that accurately reproduces the lagoon alkalinity TA_L measurements (see sections 2.4 and 3.3) is a three step time series with constant $NEC_B = 70$ mmols m^{-2} day^{-1} from 1991 to 1998, declining to a constant $NEC_B = 35$ mmols m^{-2} day^{-1} from 1999 to 2012, and declining again to $NEC_B = 25$ mmols m^{-2} day^{-1} from November 2013 to 2015.

2.4. Model Validation

A fundamental assumption of the model is that the tide-gauge sea level measurements provide an accurate estimate of the transport *U* across the barrier reef. Comparisons of *U* estimated from tide-gauge sea level measurements using Equation A1 (Appendix) with direct measurements using collocated current profilers and pressure sensors over the barrier reef indicate reasonable agreement for three different deployments

Table 1
Linear Regression Analysis Comparing Modeled to Observed Cross-Reef Transport During Three Instrument Deployments

Deployment	Correlation	Slope	Intercept (m^2/s)	Days
April 2012	0.70	0.67 ± 0.07	−0.03 ± 0.03	5
November 2013	0.73	0.50 ± 0.03	−0.01 ± 0.01	5
January 2015	0.69	0.59 ± 0.02	0.11 ± 0.01	32

Note. Correlations are significantly different from zero at the 95% confidence level. Slopes and intercepts include 95% confidence intervals.

(Figure 3 and Table 1). To what extent the differences are due to inaccuracies in the model versus differences between the along-reef average (model) and a single location on the reef (observations) is unclear. In either case, the agreement supports the use of the tide gauge sea level measurements to make long-term estimates of the tidal transport across the barrier reef.

Lagoon salinities from the model agree well with the measured lagoon salinities (Figures 5b and 6 and Table 2). Correlations between model and measured lagoon salinities are higher (0.88 and 0.90) than the correlation (0.75) between the monthly climatology and measured ocean salinities, suggesting that the accuracy of the monthly ocean salinities is a source of uncertainty in the model results. For example, in early 1998, the monthly climatology does not reproduce the anomalously high ocean salinities observed near Palau and as a result the model underestimates the lagoon salinities (Figure 6). The model also accurately reproduces the measured ocean-lagoon salinity differences (Figure 5c and Table 2). The agreement between the model and measured lagoon salinities with no adjustable parameters indicates that the model provides an accurate representation of the exchange between the ocean and the lagoon and the associated lagoon residence times.

The model with the three step NEC_B reproduces the lagoon TA, nTA, and most importantly ΔnTA measurements with remarkable accuracy (Figures 7 and 8 and Table 3). The one notable exception is April 2012 which is not included in the analyses (Table 3) because it is clearly anomalous for reasons discussed in section 4.3. Differences between the model results and the measurements range from −19 to 23 μmols kg^{-1} for TA, −18 to 9 μmols kg^{-1} for nTA and ±8 μmols kg^{-1} for ΔnTA. The larger range for TA relative to nTA is due primarily to inaccuracies in the model salinities. The larger range for nTA relative to ΔnTA is primarily because the climatological estimate of nTA for the ocean input into the model does not reproduce the rise in the measured ocean nTA in 2013–2015 (discussed in section 4.1). The correlation between the model and observed lagoon TA (0.88) is higher than the correlation between the observed ocean TA and the ocean TA estimated from Equation 6 using the climatological salinities (0.81), again suggesting that the accuracy of ocean TA estimates is a limitation in accurately modeling the lagoon TA.

The motivation for a three step time series of NEC_B is clear from the ΔnTA observations in Figure 7c. The model using a three step NEC_B provides a much better representation of the measured ΔnTA than a constant NEC_B (compare red circles to green and blue lines; Figure 7c). Using the three step NEC_B, the differences between the measured and modeled ΔnTA do not exhibit any obvious trends or patterns. In summary, the remarkable agreement between the model results and the observations supports the use of the model to interpret the sparse measurements, to determine the processes controlling variations in the lagoon TA and salinity, and to infer NEC for the barrier reef-lagoon system.

3. Results

3.1. Lagoon Residence Time

A key characteristic determining the lagoon salinity and TA variability is the residence time—the length of time ocean water transported to the bottom of the lagoon stays in the lagoon before it rises to the surface and is transported out of the lagoon. The longer the residence time the larger the TA or salinity difference between the ocean and the lagoon. For this system, the residence time is related to the adjustment time for the lagoon to reach steady state. For a constant amplitude tide (no spring-neap variation) and constant freshwater flux or NEC, the model lagoon salinity or TA approaches a steady state over a roughly exponential time scale of

$$t_{adj} = \Delta t \frac{h_L}{(\Delta\eta - h_S A_R/A_L)} \quad (7)$$

where $\Delta t \approx 0.52$ days is the duration of a tidal cycle. Model simulations indicate that the lagoon salinity or TA reaches ~65% of its steady state value after t_{adj} days and ~95% of its steady state value after $3t_{adj}$ days.

Table 2
Linear Regression Analysis Comparing Climatological and Observed Ocean Salinity and Modeled to Observed Lagoon Salinity

Variable	Correlation	Slope	Bias
S_O	0.75	0.77 ± 0.41	−0.01 ± 0.05
S_L	0.88	1.01 ± 0.33	0.06 ± 0.05
S_L Morimoto	0.90	1.42 ± 0.20	−0.03 ± 0.04
S_O-S_L	0.71	0.80 ± 0.47	−0.07 ± 0.03

Note. There are 15 values for all comparisons except Morimoto et al. (2002) (53 values near the tide gauge). Correlations are significant at the 95% confidence level. Slopes and biases include 95% confidence intervals.

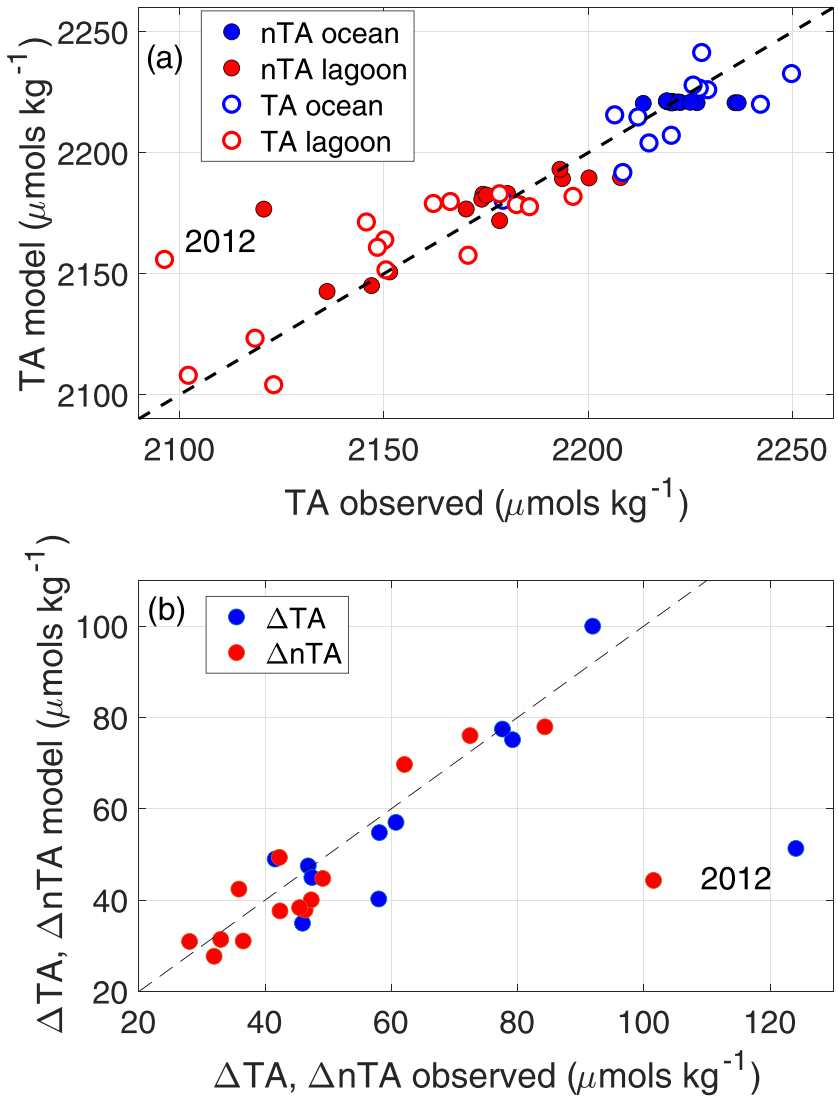

Figure 8. Comparisons of observed and modeled lagoon (a) *TA* and *nTA* (red) and (b)Δ*TA* and Δ*nTA*. The 2012 outlier is noted. Also shown in (a) is observed ocean *TA* and *nTA* compared to estimates from Equation 6 using climatological salinities (blue). Dashed lines are 1:1 lines.

Table 3
Linear Regression Analysis Comparing Climatological and Observed Ocean TA and nTA and Modeled and Observed Lagoon TA and nTA

Variable	Correlation	Slope	Bias
TA_O	0.81	0.86 ± 0.46	−5 ± 3
TA_L	0.89	0.87 ± 0.28	1 ± 5
TA_O-TA_L	0.93	0.76 ± 0.23	−3 ± 7
nTA_O	−0.24	-	−3 ± 2
nTA_L	0.93	1.11 ± 0.28	−3 ± 5
nTA_O-nTA_L	0.94	0.89 ± 0.21	0 ± 4

Note. There are 14 values because the 2012 outlier is excluded. Correlations are significantly different from zero at the 95% confidence level except for nTA_O. Slopes and biases include 95% confidence intervals.

The adjustment time (Equation 7) depends inversely on the strength of the tide ($\Delta\eta$). In Palau's Southern Lagoon, there is a substantial spring-neap variation (period of approximately 2 weeks) in the tidal transport and sea level (Figures 3 and 9a) and consequently a spring-neap variation in the adjustment time scale. Because the adjustment time scale for the lagoon (~10 days) is similar to the spring-neap time scale (~14 days) over which the adjustment time scale is changing, an instantaneous value of the adjustment time scale given by Equation 7 is not representative of the overall lagoon residence time. Consequently, the residence time is defined here as the cumulative time it takes for the model tidal exchange to replace the entire lagoon volume. This residence time ranges from ~8 days centered on the spring tide to ~14 days centered on the neap tide (Figure 9b), with a mean value of 11.5 days (slightly longer than the 10 day estimate in section 2.1). During spring tides (e.g., Figure 9c, red dashed line), when exchange is enhanced, the *TA* or salinity difference between

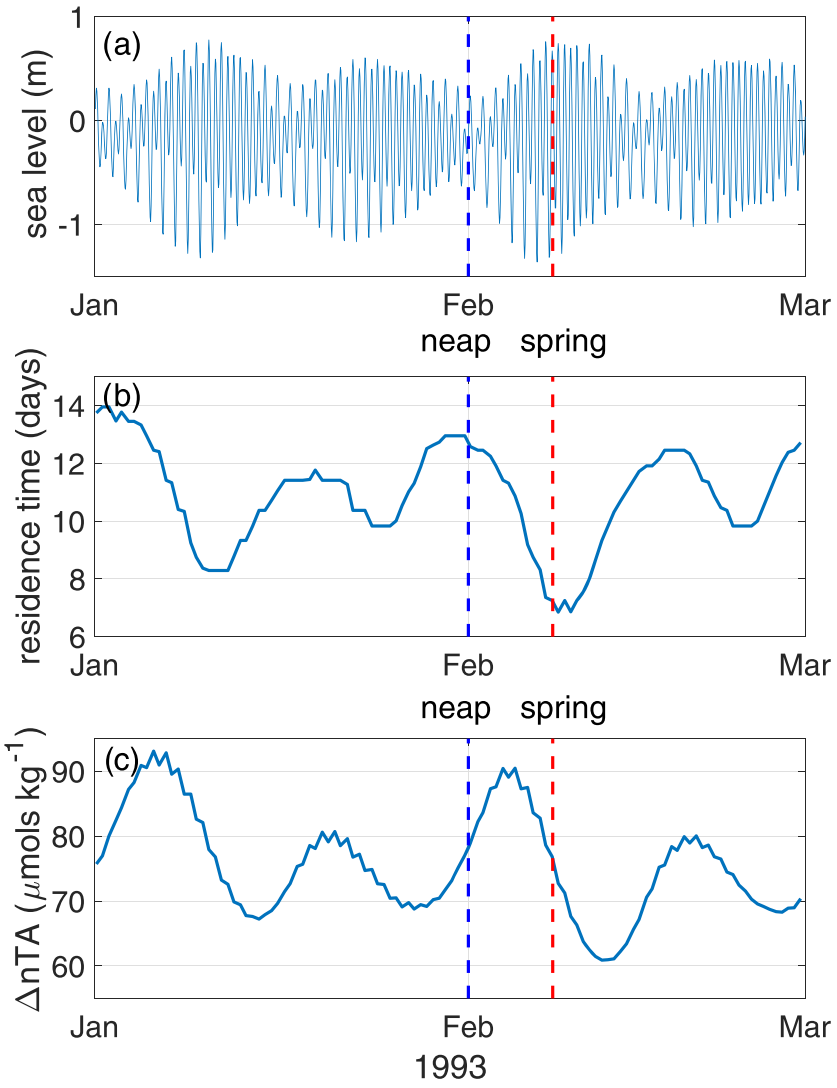

Figure 9. Time series of (a) sea level variation, (b) lagoon residence time, and (c) model estimate of lagoon Δ*nTA* for 2 months in 1993 when *NEC* and ocean *nTA* are constant. Spring-neap variations in tidal exchange result in spring-neap variations in residence time and hence in rate of change of Δ*nTA*.

the ocean and the lagoon decreases. The minimum difference between the ocean and lagoon lags behind the spring tide by a few days because they depend on the tidal exchange or residence over the previous one to 2 weeks. During neap tides (Figure 9c, blue dashed line), when exchange is reduced, the *TA* or salinity difference increases, and the maximum difference between the ocean and lagoon lags the neap tide by a few days. Consequently, there are substantial spring-neap variations in the difference between the ocean and lagoon *TA* or salinity, even when the *NEC* or freshwater flux are constant.

3.2. Salinity Variations

Precipitation is the primary driver of salinity variations in Palau's Southern Lagoon and in the adjacent ocean. The average precipitation rate (0.3 m/month) in the region is almost three times larger than the average evaporation rate (0.12 m/month) (Figure 5a). Precipitation varies substantially on daily to annual time scales, with monthly rates ranging from 0.01 to 0.86 m/month over the study period. Consequently, there are several periods when evaporation exceeds precipitation, including preceding the 1998 and 2010 El Niños.

Ocean salinities in the region from the monthly climatology vary between 33.5 and 34.5 psu on time scales of months to years (Figure 5b). Regional salt budgets indicate ocean salinity variations near Palau are primarily

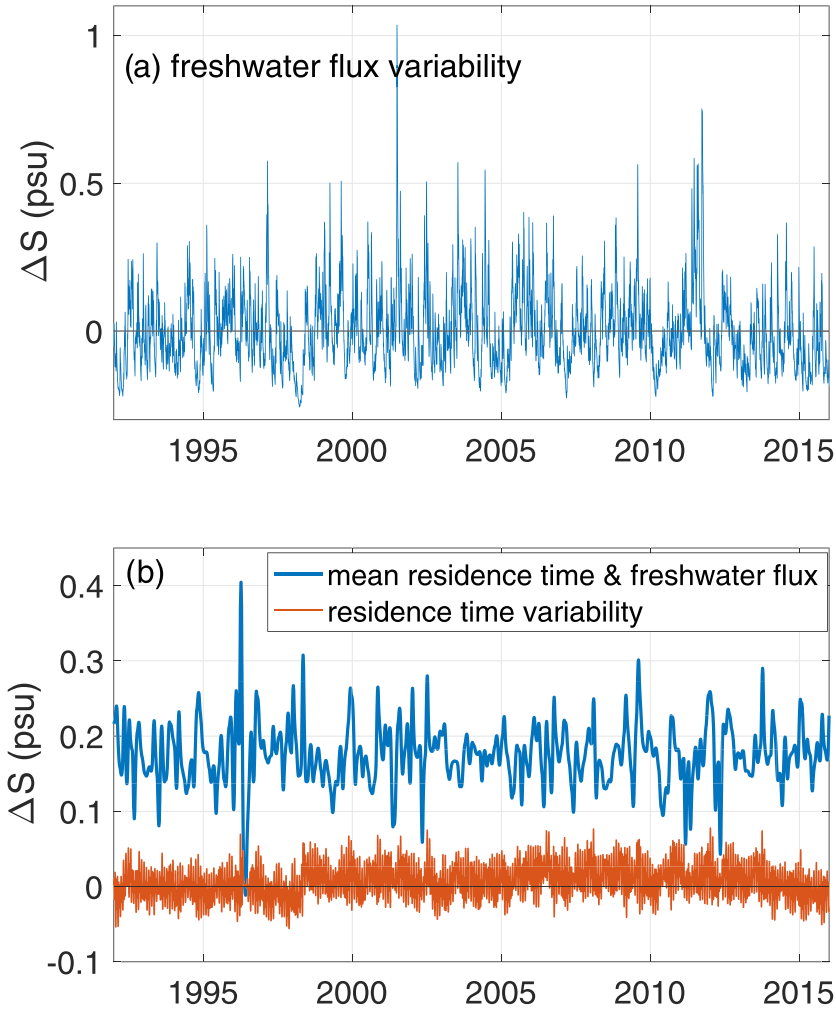

Figure 10. Time series of the contributions to the lagoon-ocean salinity difference variability from (a) variations in freshwater flux and (b) the mean residence time and mean freshwater flux (blue) and the spring-neap variations in residence time (red). Note change of scale between panels (a) and (b).

due to local precipitation (compare Figures 5a and 5b, blue lines) and to a lesser extent horizontal advection and vertical mixing (e.g., Gao et al., 2014).

Lagoon salinities, both observed and modeled, tend to track ocean salinities on time scales of months and longer, but the lagoon is consistently less salty than the ocean (Figure 5b). Salinity differences between the ocean and the lagoon range from slightly less than zero (lagoon is saltier than the ocean) to a maximum of ~1 psu (Figure 5c) and are associated with variations in precipitation. For example, high rainfall in August 1999 resulted in a lagoon salinity of 32.8 psu, ~0.75 psu less than the ocean salinity (Figure 6). While, during droughts when evaporation exceeds precipitation, for example, April 1992 and early 1998, the lagoon was saltier than the ocean (Figure 5c and 6).

The model (Equation 3) indicates that ocean-lagoon salinity differences ΔS are driven by three processes (Figure 10).

1. The mean tidal exchange rate acting on the mean freshwater flux is the reason the lagoon is on average 0.18 psu less salty than the ocean (Figures 5c and 10b, blue line). The mean tidal exchange and freshwater flux also drive fluctuations in ΔS of about $\pm$0.1 psu because of the ~3 day lag between the time varying ocean salinity and the lagoon response associated with the average lagoon residence time (as seen for ΔnTA in Figure 9c).

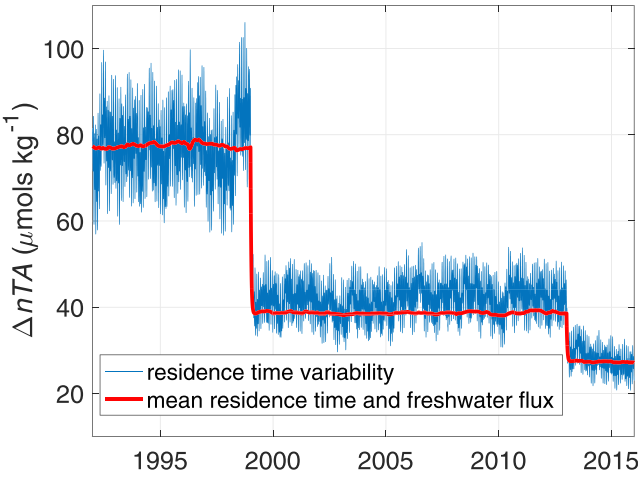

Figure 11. Time series of the contributions to model Δ*nTA* from the mean residence time (red) and from variations in residence time (blue).

2. Fluctuations in net freshwater flux, primarily precipitation (Figure 5a), drive the largest fluctuations in Δ*S* (Figure 10a) with differences ranging from −0.2 to over 1 psu.
3. Spring-neap variations in tidal exchange drive relatively small fluctuations in the salinity difference (±0.05 psu) (Figure 10b, red line).

3.3. Total Alkalinity

The model and observations indicate that variations in Southern Lagoon *TA* are due to variations in (1) ocean *TA*, (2) freshwater flux (precipitation, evaporation, and river runoff), (3) residence time, and (4) calcification, NEC_B.

Ocean *TAs* offshore of Palau's barrier reef vary by as much as 70 μmols kg^{-1} on time scales from months to years (Figure 7a, blue). The agreement between measured *TA* offshore of the barrier reef and *TA* inferred from the climatological salinity using Equation 6 indicates that regional values inferred from salinity can be used to estimate ocean *TA* near Palau (though see section 4.1). Measured ocean *nTAs* are approximately constant, ~2,220 μmols kg^{-1} (Figure 7b, blue circles), supporting the assumption (Equation 6) that ocean *TA* variability is almost entirely due to salinity variability.

Measured and modeled lagoon *TA* varies by as much as 100 μmols kg^{-1} on time scales of days to years (Figure 7a, red) with a clear dependence on ocean *TA* at monthly and longer time scales, that is, time scales longer than the lagoon residence time. Freshwater fluxes that drive variations in Δ*S* (section 3.2) result in ocean-lagoon *TA* differences (Δ*TA*) that typically range from −10 to 20 μmols kg^{-1} with occasionally larger values during strong precipitation events (not shown). The freshwater flux driven variations in lagoon *TA* or Δ*TA* are due to dilution and hence are removed by normalizing *TA* to a constant salinity, that is, *nTA* or Δ*nTA* (Figures 7b and 7c).

Variability in *nTA* and Δ*nTA* (Figures 7b and 7c) is entirely due to variations in residence time and changes in NEC_B (Figure 11). In contrast to salinity, variations in the lagoon residence time drive large variations in Δ*nTA* (and *nTA*), ~25% of the mean Δ*nTA* (Figure 11). The residence time variations (Figure 11, blue line) include spring-neap tidal variations and longer period variations associated with sea level fluctuations changing the volume of lagoon water left over the barrier reef ($A_R h_s / A_L h_L$ term in Equation 4). As noted previously, Δ*nTA* is smaller following spring tides and larger following neap tides (Figure 9c). The magnitude of the spring-neap variations in Δ*nTA* depends on NEC_B since this determines the rate of change in *TA* over the residence time (Figure 11). Prior to 1998, when NEC is large (70 mmols m^{-2} day^{-1}), the model Δ*nTA* range is ~40 μmols kg^{-1}. Between 1999 and 2012, when NEC is half the earlier value (35 mmols m^{-2} day^{-1}), the Δ*nTA* range is also about half, ~20 μmols kg^{-1} (Figure 11). The sparse observations do not resolve the spring-neap variations in Δ*nTA* seen in the model (Figure 7c). However, spring-neap variations in lagoon residence time do account for some of the observed variability, most notably the model indicates that the apparent increase in measured lagoon *nTA,* and decrease in Δ*nTA*, from 1992 to 1998 (Figures 7b and 7c, red symbols) is not due to a decline in NEC_B, but rather is a consequence of sampling at the maximum of the spring-neap cycle in 1992 and at the minimum of the spring-neap cycle in early 1998.

The agreement between the model and the observations (Figure 7c) supports the assumption that NEC_B was approximately constant at 70 mmols m^{-2} day^{-1} from 1992 to 1998, decreased to a constant 35 mmols m^{-2} day^{-1} from 1998 to 2011, and decreased again to a constant 25 mmols m^{-2} day^{-1} from 2012 to 2015. The first decline occurred sometime between February 1998 and 1999 and is associated with loss of coral cover following a coral bleaching event in the fall of 1998 (Bruno et al., 2001; Kayanne, 2007; Watanabe et al., 2006). The observations and model suggest the second decline in NEC_B occurred sometime between October 2011 and 2013 and the cause of this decline is less clear (see section 4.5).

The inferred NEC_B is for the combined barrier reef and Southern Lagoon system. NEC_L for just the Southern Lagoon can be estimated from Equation 5 given independent estimates of NEC_R. Previous studies indicate that NEC_R was 130 mmols m^{-2} day^{-1} in July 1994, 74 mmols m^{-2} day^{-1} in September 2000 (Kayanne

et al., 2005), and 99 mmols m^{-2} day^{-1} from measurements made in April 2012, November 2013, and January 2015, respectively (Shamberger et al. in prep). Using these NEC_R estimates and the corresponding NEC_B values in Equation 5 averaged over the residence time when the samples were taken, the resulting Southern Lagoon NEC_L estimates are 47 mmols m^{-2} day^{-1} for July 1994, 24 mmols m^{-2} day^{-1} for September 2000, and 11 mmols m^{-2} day^{-1} for 2012–2015. Thus, both the lagoon and the barrier reef experienced roughly a 45% reduction in *NEC* between 1994 and 2000 (Watanabe et al., 2006), presumably associated with the loss of coral following the 1998 bleaching event. Between 2000 and 2012–2015 the barrier reef experienced a ~30% recovery in *NEC*, but the lagoon *NEC* declined by a further 55% resulting in the 30% decline in NEC_B for the combined lagoon and barrier reef system.

4. Discussion

4.1. Ocean *TA* in Vicinity of Palau

Prior to 2013, the ocean near-surface *nTA* observations near Palau are consistently lower (mean difference 13 μmols kg^{-1}) than open ocean observations from the equatorial northwestern North Pacific (0°–15°N and 120°–150°E) (Figure 7b) and relative to empirical relationships for the equatorial Pacific (e.g., Lee et al., 2006), presumably because of the influence of Palau's coral reefs on the surrounding ocean (Cyronak et al., 2018). Interestingly, the observed ocean *nTA*s from 2013 to 2015 are higher than the pre 2013 *nTA*s and consequently closer to the open ocean *nTA*s, suggesting either Palau is having less impact on the surrounding ocean or there was a shift in the regional circulation that moved oceanic water close to the barrier reef on the southwest side of Palau after 2013. Note that the ocean water samples from 2012 to 2015 were generally taken closer to the barrier reef than the prior water samples which should result in anomalously lower, not higher, *nTA* values.

4.2. The Impact of the Salt Balance on Ocean-Lagoon Exchange

The lagoon salinity variability and the processes controlling it are critical to understanding the variations in the lagoon water chemistry because the ocean-lagoon salinity difference is fundamental to the nature of the ocean-lagoon exchange. Normally, precipitation exceeds evaporation, the lagoon is less salty than the ocean, and the tidal exchange is as described in section 2.1 (Figure 4), with salty ocean water sinking to the bottom of the lagoon on the flood tide. However, during extreme droughts in Palau, when evaporation exceeds precipitation for long enough that the lagoon is saltier than the ocean (e.g., 1992; Figure 5), the exchange process would be different. In this case, since the ocean water is not denser than the lagoon water, it will not fall to the bottom of the lagoon and the exchange may be limited to near-surface water. This might lead to a temporary isolation of the deeper lagoon water and a change in the lagoon residence time. It is noteworthy that extreme droughts with lagoon salinity exceeding ocean salinity preceded both the 1998 and 2010 El Niño's (Figure 5). While not typical, the model results indicate lagoon salinities are greater than or equal to oceanic salinities about 10% of the time, as also suggested by the observations from 1992 to 2002 (Figure 5c) and mid 1998 (Figure 6). It is unclear how droughts (low precipitation) combined with a resulting change in the ocean-lagoon exchange process influences the coral reefs of Palau's numerous large and small lagoons.

4.3. April 2012 Anomaly

The April 2012 lagoon *TA* observation is clearly an outlier (Figures 2, 7, and 8). The 2012 measurements are not actually from the lagoon but from a site on the barrier reef near the lagoon edge. However, numerous samples at this site during the ebb tide (when water flows from the lagoon toward the ocean) all indicate consistently low *nTA* relative to both the ocean and all other lagoon *nTA* measurements after 1998. The low *nTA* in 2012 may be the result of a band of surface lagoon water that passed back and forth across the barrier reef several times without mixing with deeper lagoon water or being swept away from the outer edge of the lagoon. A clear example of this process occurred on 6 April when near-surface lagoon water initially swept onto the barrier reef during the ebb tide had a lower *nTA* when it was swept back to the lagoon on the flood tide presumably due to further calcification over the barrier reef (Figure 12). The decrease in *nTA* at the onset of the flood tide 14:00–16:00 6 April was about 30 μmols kg^{-1} which is very close to the expected value of 32 μmols kg^{-1} using the barrier reef $NEC_R = 99$ mmols m^{-2} day^{-1} (Shamberger et al. in prep) and the 6 hr residence time over the barrier reef ($\Delta nTA = 2NEC\, t_{res}/\rho h_r$). This process also occurred on 4 and 5 April but the decreases in *nTA* at the onset of the flood tide were smaller (15 and 7 μmols kg^{-1}). The decrease in *nTA*

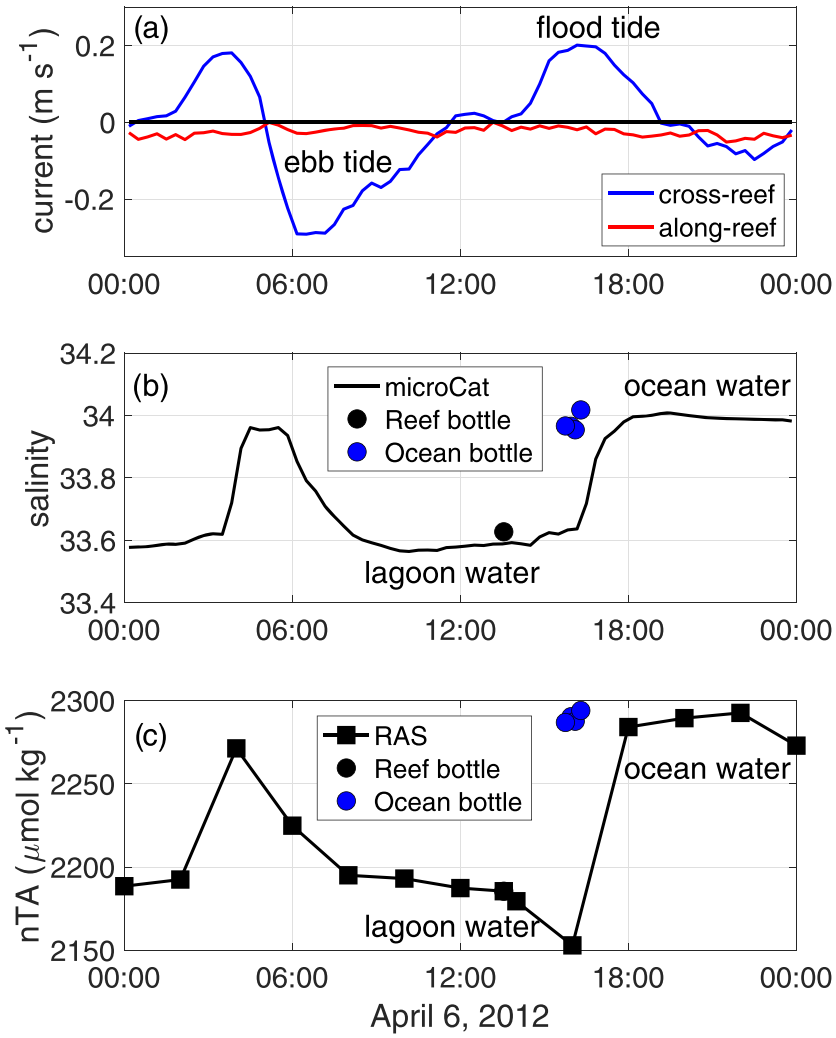

Figure 12. Time series for 6 April 2012 of (a) depth-averaged cross-reef and along-reef currents, (b) salinity, and (c) *nTA* from instruments deployed at a site over the barrier reef near the lagoon. Reef bottle samples were taken at the instrument site and ocean bottle samples just offshore of the barrier reef. Ebb tides (flow toward the ocean) carry low salinity and *nTA* lagoon water over the barrier reef, while flood tides transport high salinity and *nTA* ocean water toward the lagoon. Note that the decline in the lagoon water *nTA* at the start of the flood tide is from 14:00 to 16:00 UTC.

on 6 April is about half of the ΔnTA anomaly of ~60 μmols kg^{-1} for April 2012 (Figures 7c and 8c) suggesting only a few tidal cycles would be required to generate the anomaly. This process may also explain the low lagoon *nTA* near the barrier reef in the April 2000 cross section (Figure 4b) of Watanabe et al. (2006). This mechanism may contribute to the reduced near-surface *TA* in the lagoon.

4.4. *NEC* Comparisons to Previous Studies

The residence times from the tidal exchange model, 8–14 days (section 3.1), are shorter than the residence times used by Watanabe et al. (2006) which ranged from 18 to 30 days. The agreement between the model with no free parameters and observed salinities (section 2.4; Table 2 and Figures 5 and 6) supports the shorter model residence times. As a result of the shorter residence times, the lagoon *NEC* values reported here (48 mmols m^{-2} day^{-1} in 1994 and 23 mmols m^{-2} day^{-1} in 2000) are larger than the corresponding values (~19 mmols m^{-2} day^{-1} in 1994 and 10–19 mmols m^{-2} day^{-1} in 2000) estimated by Watanabe et al. (2006).

The estimated Southern Lagoon NEC_L of 24 mmols m^{-2} day^{-1} for September 2000 and 11 mmols m^{-2} day^{-1} for 2013–2015 is similar to estimates for a much smaller inner lagoon (Risong) in Palau of 16 mmols m^{-2} day^{-1} in March 2012 and 36 mmols m^{-2} day^{-1} in November 2013 (Shamberger et al., 2018) and

estimates for a back reef in Palau of 33.8 mmols m^{-2} day^{-1} in April 2011 (Teneva et al., 2013). The surface area of the Southern Lagoon (500 km^2) is 4,000 times larger than Risong Lagoon (12,535 m^2). Despite the difference in size, Risong Lagoon residence times (7–14 days) are similar to the Southern Lagoon because the length of the barrier reef is 3,000 times larger than the width of the channel (28 m) that flushes Risong Lagoon (water depths and tidal currents are similar).

The NEC_L estimates for the Southern Lagoon, both prior to and after the 1998 bleaching event, are on the low end for coral reef systems where *NEC* has been estimated (e.g., DeCarlo et al., 2017) but are roughly in the range cited by Smith and Kinsey (1976) for protected lagoon environments (22 ± 11 mmols m^{-2} day^{-1}). In Palau, the lower *NEC* in the Southern Lagoon and Risong Lagoon relative to the barrier reef is not due to coral cover which is higher or similar in the inner lagoons (Barkley et al., 2015). The difference in *NEC* may be, at least partially, due to differences in relative growth rates of the barrier reef and lagoon corals. For *porites* average growth rates were 1.31 ± 0.42 gm cm^{-2} $year^{-1}$ over the barrier reef and 0.85 ± 0.423 gm cm^{-2} $year^{-1}$ in the lagoons (Barkley & Cohen, 2016).

4.5. *NEC* Decline and Lack of Recovery

The 45% decline in NEC_B sometime between February 1998 and 1999 has been attributed to a loss of coral and possibly other calcifiers following the 1998 bleaching event caused by anomalously warm sea surface temperatures (Bruno et al., 2001; Kayanne, 2007; Watanabe et al., 2006). While coral cores from Palau exhibited stress bands during the 1998 bleaching events, there was no obvious decline in coral growth rates after these events (Barkley & Cohen, 2016) supporting the assumption that the loss of coral (calcifier) cover caused the decline in *NEC*.

The cause of the further decline in NEC_B to 25 mmols m^{-2} day^{-1} sometime between October 2011 and 2013 is less clear. It does not appear to be due to the 2010 bleaching event (e.g., Barkley & Cohen, 2016; van Woesik et al., 2012) since the ΔnTA in September 2011 is essentially the same as for the period from 1999 to 2002, though this conclusion is based on only the September 2011 measurements. It is also possible that the lower observed values of ΔnTA for 2013–2015 are a consequence of the proximity of those lagoon samples to the barrier reef leading to an oceanic influence that is not representative of the broader lagoon. However, there is not an obvious salinity anomaly supporting an oceanic influence on the 2013–2015 lagoon samples.

Interpretation of the separate changes in *NEC* over the barrier reef and in the Southern Lagoon is challenging because there are only three estimates of NEC_R, and hence, NEC_L separated by 6 (1994–2000) and ~13 years (2000–2013). The ~50% decline in both NEC_R and NEC_L from 1994 to 2000 are consistent with the decline in coral (calcifier) cover, suggesting the 1998 bleaching event had a similar impact on the barrier reef and Southern Lagoon (Watanabe et al., 2006). In contrast, between 2000 and 2013, the NEC_R estimate indicates the barrier reef recovered somewhat, while the NEC_L estimate indicates the Southern Lagoon declined further. The barrier reef recovery is puzzling because two cross-reef surveys indicate a further decline in coral cover between 2000 and 2015 (Kayanne, 2007, transect data provided by M. Gouezo Palau International Coral Reef Center), and there was no significant change in coral growth rates over the barrier reef from cores spanning 1990–2012 (Figure 5; Ngerdiluches panel in Barkley & Cohen, 2016). The cause of the further decline in NEC_L for the Southern Lagoon is not known but is a concern given the low calcification rate and suggests the need for more frequent monitoring.

Watanabe et al. (2006) noted that the barrier reef-Southern Lagoon system and the Southern Lagoon alone had not recovered from the 1998 bleaching event as of 2002. The recent 2011–2015 ΔnTA measurements (Figure 7c) and associated *NEC* estimates indicate that the barrier reef-Southern Lagoon system and the Southern Lagoon alone have still not recovered as of 2015, nearly two decades after the 1998 bleaching event. Though *NEC* cannot be inferred for the data gap between 2002 and 2011, it seems unlikely that the system would have recovered and then returned to the same NEC_B in 2011 as in 1999 to 2002.

5. Summary

Total alkalinity (*TA*) variability in Palau's largest coral reef lagoon (Southern Lagoon) is examined using sparse observations collected from the lagoon and ocean during studies spanning 1992–2002 and 2011–2015 (Figure 2) combined with a model of *TA* variability driven by tidal exchange across the

barrier reef separating the lagoon from the ocean. The key feature of the model is that saltier (denser) ocean water is transported across the barrier reef on the flood tide and sinks to the bottom of the less salty (dense) lagoon (Figure 4), replacing less dense near-surface lagoon water that is transported offshore to the ocean on the ebb tide.

Based on the model, lagoon residence times vary from 8 days during spring tides to 14 days during neap tides (Figure 9). The model accurately reproduces the observed variations in the lagoon salinity with no free parameters (Figures 5 and 6 and Table 2), supporting the use of the model to interpret the sparse measurements. The mean salinity difference between the ocean and the lagoon, which plays a fundamental role in the tidal exchange, is set by the mean precipitation exceeding evaporation and the residence time of the lagoon (Figure 10b). Variability in the ocean-lagoon salinity difference on time scales of days to years is primarily due to the large variations in Palau's precipitation (Figure 5 and 10a).

Lagoon *TA* variability is partly driven by variations in ocean *TA* (range ~50 μmols kg^{-1}; Figure 7a) and in precipitation and evaporation (range −20 to 10 μmols kg^{-1}), both of which can be removed by considering *TA* normalized to a constant salinity (*nTA*) (Figure 7b). The remaining variability in *nTA* and the ocean-lagoon difference Δ*nTA* is caused by variations in *NEC* and variations in the lagoon residence times. Spring-neap variations in residence time drive large variations in Δ*nTA* (range up to 40 μmols kg^{-1}; Figure 11) with Δ*nTA* decreasing during spring tides and increasing during neap tides (Figure 9c). This means that changes in Δ*nTA* cannot be interpreted as indicative of changes in *NEC* without first considering when in the tidal cycle samples were collected, as shown for the apparent decrease in Δ*nTA* from 1992 to 1998 (section 3.3).

The remarkable agreement between the model and the measurements of the lagoon *nTA* and Δ*nTA* (Figures 7 and 8 and Table 3) indicates that the net ecosystem calcification rate for the combined barrier reef and Southern Lagoon system (NEC_B) was a constant 70 mmols m^{-2} day^{-1} from 1992 to 1998, declined to a constant 35 mmols m^{-2} day^{-1} from 1999 to 2012, and declined again to a constant 25 mmols m^{-2} day^{-1} from 2013–2015. Based on independent estimates of *NEC* for the barrier reef, *NEC* for the Southern Lagoon alone declined by ~50% from 47 mmols m^{-2} day^{-1} in July 1994 to 24 mmols m^{-2} day^{-1} in September 2000 and by an additional 55% to 11 mmols m^{-2} day^{-1} in 2013–15. The 50% decline in *NEC* in 1998 for both the combined barrier reef-lagoon system and the lagoon alone is due to a loss of coral cover associated with a severe bleaching event (e.g., Bruno et al., 2001; Kayanne, 2007; Watanabe et al., 2006). The cause of the subsequent decline in sometime between October 2011 and October 2013 and in the Southern Lagoon alone between 2000 and 2013 is not known. The *NEC* estimates indicate that as of 2015, Palau's largest lagoon-barrier reef system has not recovered from the 1998 bleaching event that caused a severe loss of coral cover.

Appendix A: Model Derivation

The volume budget for the lagoon is

$$A_L \frac{\partial \eta_L}{\partial t} = L_R U + A_L(P - E) + R \tag{A1}$$

where A_L is the surface area of the lagoon, η_L is the spatially average sea level variation over the lagoon, L_R is the length of the barrier reef, U is the cross-reef transport (per unit length) at the lagoon edge of the barrier reef, P and E are the precipitation and evaporation rates over the lagoon, and R is the river runoff into the lagoon. Equation A1 states that temporal changes in the lagoon volume are equivalent to the rate of change of sea level times the surface area of the lagoon and are caused by cross-reef transport of water in and out of the lagoon, the net freshwater flux into the lagoon at the sea surface and river runoff into the lagoon. Transport through channels on the eastern side of the lagoon is neglected. The dominant cause of sea level changes in the lagoon is the tidal exchange because $(P - E) \ll \partial\eta/\partial t$—changes in sea level over a tidal cycle are ~1 m (Figure 7a) and precipitation minus evaporation rates are order 1 cm day^{-1} (Figure 5a). Integrating Equation 8 from the start to the end of the flood (ebb) tide gives the net volume transport into (out of) the lagoon

$$Q_F = \int_{t_s}^{t_e} L_R U dt = A_L \Delta\eta - [A_L(P - E) + R]\Delta t/2 \tag{A2}$$

where $\Delta\eta = \eta(t+\Delta t/2) - \eta(t)$ is the change in the sea level from the start to the end of the flood (positive) or ebb tide (negative) and Δt is the duration of a full tidal cycle.

Based on the conceptual model, we are interested in the volume of ocean water that makes it to the lagoon during flood tide and then sinks to the bottom of the lagoon (Figure 4). However, at the start of the flood tide (end of the ebb tide), the barrier reef is typically covered with lagoon water that is transported back into the lagoon on the flood tide prior to the ocean water entering the lagoon. The volume of lagoon water transported into the lagoon during the flood tide is

$$Q_{FL} = A_R h_s \tag{A3}$$

where A_R is the area of the barrier reef and h_S is the water depth over the barrier reef at the start of the flood tide. Subtracting this volume of lagoon water from the total volume of water entering the lagoon (Equation A2) yields the volume of ocean water entering the lagoon during the flood tide given in Equation 1. Only lagoon water is transported out of the lagoon on the ebb tide because the ocean water sinks to the bottom of the lagoon so

$$Q_E = A_L \Delta\eta - [A_L(P-E) + R]\Delta t/2 \tag{A4}$$

The net volume of lagoon water transported offshore over a tidal cycle is Q_E minus Q_{FL} the lagoon water transported in on the ebb tide given in Equation 2 (noting that positive values are into the lagoon).

The lagoon salt balance is

$$\frac{\partial}{\partial t}\left(V_L S_L^A\right) = V_L \frac{\partial S_L^A}{\partial t} + S_L^A \frac{\partial V_L}{\partial t} = -L_R U S \tag{A5}$$

where S_L^A is the volume averaged lagoon salinity and S is the salinity at the seaward side of the lagoon. Integrating Equation A5 over a tidal cycle and using Equations 1 and 2 yields

$$\begin{aligned} V_L \Delta S_L^A = {} & (A_L \Delta\eta_F - A_R h_S)\left(S_O - S_L^A\right) + A_R h_S \left(S_L^S - S_L^A\right) \\ & + A_L \Delta\eta_E \left(S_L^S - S_L^A\right) - \left(A_L(P-E) + R\right)\left(S_O + S_L^S\right)\frac{\Delta t}{2} \end{aligned} \tag{A6}$$

Here $\Delta S_L^A = S_L^A(t+\Delta t) - S_L^A(t)$ is the change in the volume averaged lagoon salinity over a tidal cycle, and S_O and S_L^S are the near-surface ocean and lagoon salinities respectively.

Equation A6 states that the change in the average lagoon salinity over a tidal cycle is due to the import of near-surface ocean salinity and lagoon salinity to the lagoon during the flood tide, the export of near-surface lagoon salinity during the ebb tide and a reduction of the lagoon salinity due to the net surface flux of fresh water (precipitation minus evaporation and runoff). Note for simplicity we are assuming that changes in the salinity due to precipitation and evaporation as the water crosses the barrier reef are small, that is the salinity at the lagoon edge of the barrier reef equals the ocean salinity, $S_R \approx S_O$ (e.g., Figure 5a).

To estimate lagoon salinities (and TA below) from Equation A6 requires a relationship between the volume average S_L^A and near-surface S_L^S lagoon salinities. Following Watanabe et al. (2006), the simplest assumption is that the lagoon is well mixed so $S_L^S = S_L^A$, which reduces Equations A6 to 3. Alternatively, one could assume a particular salinity and alkalinity profile in the lagoon, for example, a linear profile

$$S_L^A = \left(S_L^S + S_O\right)/2 \text{ and } TA_L^A = \left(TA_L^S + TA_R\right)/2$$

as suggested in Figure 4.

The lagoon total alkalinity balance is

$$\frac{\partial}{\partial t}\left(V_L TA_L^A\right) = V_L \frac{\partial TA_L^A}{\partial t} + TA_L^A \frac{\partial V_L}{\partial t} = -L_R U\, TA + R\, TA_{river} - A_L \frac{2NEC_L}{\rho} \tag{A7}$$

TA_{river} is the alkalinity of the river runoff, NEC_L is the net ecosystem calcification rate per unit bottom area in the lagoon, and ρ is the density of sea water. The TA balance differs from the salinity balance in that the TA of the runoff is not zero and positive net ecosystem calcification reduces the lagoon ta.

Integrating over a tidal cycle using Equations 1 and 2 yields

$$V_L \Delta TA_L^A = (A_L \Delta\eta_F - A_R h_S)(TA_R - TA_L^A) + (A_L \Delta\eta_E + A_R h_S)(TA_L^S - TA_L^A) - A_L(P-E)(TA_R + TA_L^S)\frac{\Delta t}{2} - R\left((TA_R + TA_L^S) - 2TA_{river}\right)\frac{\Delta t}{2} - 2A_L NEC_L \Delta t/\rho \quad \text{(A8)}$$

where TA_R is the alkalinity of the ocean water when it reaches the lagoon edge of the barrier reef. In contrast to the salt budget we do not expect $TA_R = TA_O$ because of calcification over the barrier reef. To estimate TA_R, the change in alkalinity across the reef is estimated as

$$TA_R = TA_O - 2\frac{NEC_R}{\rho h_R} t_{res} = TA_O - 2\frac{NEC_R}{\rho h_R}\frac{W_R}{u_R} \quad \text{(A9)}$$

where NEC_R is the net ecosystem calcification rate per unit area over the barrier reef, h_R is the water depth over the reef, $t_{res} = W_R/u_R$ is the time it takes a water parcel to cross the reef (hours), $W_R \approx 1.5$ km is the width of the reef, and u_R is the average cross-reef velocity. The cross-reef transport $U_R = u_R h_R$ averaged over the flood tide from Equation 8 is

$$\frac{1}{\Delta t}\int_{t_s}^{t_e} U_R dt = \frac{Q_R}{L_R \Delta t} \approx \frac{A_L + A_R/2}{L_R}\frac{\Delta\eta_F}{\Delta t} \quad \text{(A10)}$$

which accounts for the difference in transport between the ocean and lagoon sides of the barrier reef associated with the change in sea level height but neglects the freshwater flux contributions that are small (but could be easily added). Substituting Equation A10 into Equation A9

$$TA_R \approx TA_O - 2\frac{NEC_R}{\rho}\frac{A_R}{(A_L + A_R/2)}\frac{\Delta t}{\Delta\eta_F} \quad \text{(A11)}$$

Finally, replacing TA_R in Equation A8 with Equation A11 and dividing by $V_L = A_L h_L$ yields

$$\Delta TA_L^A = (TA_O - TA_L^A)\left(\frac{\Delta\eta_F}{h_L} - \frac{A_R}{A_L}\frac{h_S}{h_L}\right) + (TA_L^S - TA_L^A)\left(\frac{\Delta\eta_E}{h_L} + \frac{A_R}{A_L}\frac{h_S}{h_L}\right) - (TA_O + TA_L^S)\frac{(P-E)}{h_L}\frac{\Delta t}{2} - \left((TA_O + TA_L^S) - 2TA_{river}\right)\frac{R}{A_L h_L}\frac{\Delta t}{2} - \frac{2\Delta t}{\rho h_L}\left\{NEC_L + NEC_R\frac{A_R}{(A_L + A_R/2)}\left(1 - \frac{A_R}{A_L}\frac{h_S}{\Delta\eta_F} - \left(\frac{P - E + PA_{WS}/A_L}{\Delta\eta_F}\right)\right)\right\} \quad \text{(A12)}$$

Again, assuming the lagoon is well mixed ($TA_L^S = TA_L^A$) and neglecting the last term, which is small, yields Equation 4.

Data Availability Statement

Total alkalinity and salinity samples from 1994 to 2002 are from Watanabe et al. (2006) and for 2011–2015 are archived at Biological and Chemical Oceanography Data Management Office at https://www.bco-dmo.org/dataset/489014/data and described in Barkley et al. (2015), DeCarlo et al. (2015), and Shamberger et al. (2014). Additional salinity data is from Morimoto et al. (2002). Malakal tide gauge data is from the University of Hawaii Sea Level Center at https://uhslc.soest.hawaii.edu (Caldwell et al., 2015). Meteorological data is from National Climate Data Center's Global Historical Climate Network and Woods Hole Oceanographic Institutions Objectively Analyzed air-sea Flux climatology (http://oaflux.whoi.edu) funded by the NOAA Climate Observations and Monitoring program at https://www.ncdc.noaa.gov/data-access/land-based-station-data/land-based-datasets/global-historical-climatology-network-ghcn website. Region temperature salinity and objectively mapped salinity are from the Met Office Hadley Centre EN4.2.1 hydrographic database at https://www.metoffice.gov.uk/hadobs/en4/download-en4-2-1.html (Good et al., 2013).

Acknowledgments

The authors thank Y. Golbuu, T. DeCarlo, K. Pietro, G.P. Lohmann, D. McCorkle, R. Belastock, K. Hoering, M. E. Gonneea, A. Helbling, A. Kealoha, and the staff of the Palau International Coral Reef Center for their assistance with fieldwork and analyses. The authors also thank A. Watanabe and H. Kayanne for their early work and data and for additional information they provided about their data. This work was partially supported by NSF award 1220529 to A.L.C., S.J.L., and K.E.F.S and NSF award 1737311 to A.L.C. and the Oceanography Department, Texas A&M University K.E.F.S.

References

Andersson, A. J., & Gledhill, D. (2013). Ocean acidification and coral reefs: Effects on breakdown, dissolution, and net ecosystem calcification. *Annual Review of Marine Science*, *5*(1), 321–348. https://doi.org/10.1146/annurev-marine-121211-172241

Barkley, H. C., & Cohen, A. L. (2016). Skeletal records of community-level bleaching in Porites corals from Palau. *Coral Reefs*, *35*(4), 1407–1417. https://doi.org/10.1007/s00338-016-1483-3

Barkley, H. C., Cohen, A. L., Golbuu, Y., Starczak, V. R., DeCarlo, T. M., & Shamberger, K. E. F. (2015). Changes in coral reef communities across a natural gradient in seawater pH. *Science Advances*, *1*(5), e1500328 (2015). https://doi.org/10.1126/sciadv.1500328

Bruno, J. F., Siddon, C. E., Witman, J. D., Colin, P. L., & Toscano, M. A. (2001). El Nino related coral bleaching in Palau, Western Caroline Islands. *Coral Reefs*, *20*(2), 127–136. https://doi.org/10.1007/s003380100151

Caldwell, P. C., Merrifield, M. A., Thompson, P. R. (2015). Sea level measured by tide gauges from global oceans—The joint archive for sea level holdings (NCEI accession 0019568), version 5.5, NOAA National Centers for environmental information, Dataset, https://doi.org/10.7289/V5V40S7W

Cyronak, T., Andersson, A. J., Langdon, C., Albright, R., Bates, N. R., Caldeira, K., et al. (2018). Taking the metabolic pulse of the world's coral reefs. *PLoS ONE*, *13*(1), e0190872. https://doi.org/10.1371/journal.pone.0190872

Davis, K. L., McMahon, A., Kelaher, B., Shaw, E., & Santos, I. R. (2019). Fifty years of sporadic coral reef calcification estimates at one tree island, great barrier reef: Is it enough to imply long term trends? *Frontiers in Marine Science*, *6*, 282. https://doi.org/10.3389/fmas.2019.00282

DeCarlo, T. M., Cohen, A. L., Barkley, H. C., Cobban, Q., Young, C., Shamberger, K. E. F., et al. (2015). Coral macrobioerosion is accelerated by ocean acidification and nutrients. *Geology*, *43*(1), 7–10. https://doi.org/10.1130/G36147.1

DeCarlo, T. M., Cohen, A. L., Wong, G. T. F., Shiah, F.-K., Lentz, S. J., Davis, K. A., et al. (2017). Community production modulates coral reef pH and sensitivity of ecosystem calcification to ocean acidification. *Journal of Geophysical Research: Oceans*, *122*, 745–761. https://doi.org/10.1002/2016JC012326

Gao, S., Qu, T., & Nie, X. (2014). Mixed layer salinity budget in the tropical Pacific Ocean estimated by a global GCM. *Journal of Geophysical Research: Oceans*, *119*, 8255–8270. https://doi.org/10.1002/2014JC010336

Good, S. A., Martin, M. J., & Rayner, N. A. (2013). EN4: Quality controlled ocean temperature and salinity profiles and monthly objective analyses with uncertainty estimates. *Journal of Geophysical Research: Oceans*, *118*, 6704–6716. https://doi.org/10.1002/2013JC009067

Hughes, T. P., Kerry, J. T., Álvarez-Noriega, M., Álvarez-Romero, J. G., Anderson, K. D., Baird, A. H., et al. (2017). Global warming and recurrent mass bleaching of corals. *Nature*, *543*(7645), 373–377. https://doi.org/10.1038/nature21707

Kayanne, H. (2007). *Landform of the Palau barrier reef, chapter 2 in coral reefs of Palau* (pp. 30–37). Koror, Palau: Palau international coral reef center.

Kayanne, H., Hata, H., Kudo, S., Yamano, H., Watanabe, A., Ikeda, Y., et al. (2005). Seasonal and bleaching-induced changes in coral reef metabolism and CO_2 flux. *Global Biogeochemical Cycles*, *19*, GB3015. https://doi.org/10.1029/2004GB002400

Kayanne, H., Yamamuro, M., & Ohta, H. (1993). Chemical composition of seawater within and around Palau barrier reef. In A. Nishimura (Ed.), *F. Y. report for elemental cycles in the ocean* (pp. 208–222). Japan, Tsukuba: Geol. Surv.

Lee, K., Tong, L. T., Millero, F. J., Sabine, C. L., Dickson, A. G., Goyet, C., et al. (2006). Global relationships of total alkalinity with salinity and temperature in surface waters of the world's oceans. *Geophysical Research Letters*, *33*, L19605. https://doi.org/10.1029/2006GL027207

Lentz, S. J., Davis, K. A., Churchill, J. H., & DeCarlo, T. M. (2017). Coral reef drag coefficients—Water depth dependence. *Journal of Physical Oceanography*, *47*(5), 1061–1075. https://doi.org/10.1175/JPO-D-16-0248.1

Maragos, J. E., & Cook, C. W. Jr. (1995). The 1991–1992 rapid ecological assessment of Palau's coral reefs. *Coral Reefs*, *14*(4), 237–252. https://doi.org/10.1007/BF00334348

Morimoto, M., Abe, O., Kayanne, H., Kurita, N., Matsumoto, E., & Yoshida, N. (2002). Salinity records for the 1997–98 El Niño from Western Pacific corals. *Geophysical Research Letters*, *29*(11), 1540. https://doi.org/10.1029/2001GL013521

Olsen, A., Key, R. M., van Heuven, S., Lauvset, S. K., Velo, A., Lin, X., et al. (2016). The Global Ocean Data Analysis Project version 2 (GLODAPv2)—An internally consistent data product for the world ocean. *Earth System Science Data*, *8*(2), 297–323. https://doi.org/10.5194/essd-8-297-2016

Perry, C. T., Alvarez-Filip, L., Graham, N. A. J., Mumby, P. J., Wilson, S. K., Kench, P. S., et al. (2018). Loss of coral reef growth capacity to track future increases in sea level. *Nature*, *558*(7710), 396–400. https://doi.org/10.1038/s41586-018-0194-z

Shamberger, K. E. F., Lentz, S. J., & Cohen, A. L. (2018). Low and variable ecosystem calcification in a coral reef lagoon under natural acidification. *Limnology and Oceanography*, *63*(2), 714–730. https://doi.org/10.1002/lno.10662

Shamberger, K. E. F., Cohen, A. L., Golbuu, Y., McCorkle, D. C., Lentz, S. J., & Barkley, H. (2014). Diverse coral communities in naturally acidified waters of a western Pacific reef. *Geophysical Research Letters*, *41*, 499–504. https://doi.org/10.1002/2013GL058489

Silverman, J., Kline, D. I., Johnson, L., Rivlin, T., Schneider, K., Erez, J., et al. (2012). Carbon turnover rates in the one tree island reef: A 40-year perspective. *Journal of Geophysical Research*, *117*, G03023. https://doi.org/10.1029/2012JG001974

Silverman, J., Lazar, B., & Erez, J. (2007). Effect of aragonite saturation, temperature, and nutrients on the community calcification rate of a coral reef. *Journal of Geophysical Research*, *112*, C05004. https://doi.org/10.1029/2006JC003770

Silverman, J., Schneider, K., Kline, D. I., Rivlin, T., Rivlin, A., Hamylton, S., et al. (2014). Community calcification in Lizard Island, great barrier reef: A 40-year perspective. *Geochimica et Cosmochimica Acta*, *144*, 72–81. https://doi.org/10.1016/j.gca.2014.09.011

Smith, S. V., & Kinsey, D. W. (1976). Calcium carbonate production, coral reef growth, and sea level change. *Science*, *194*(4268), 937–939. https://doi.org/10.1126/science.194.4268.937

Suzuki, A. (1995). Carbon cycle in the coral reef ecosystems. Ph. D. thesis Tohoku Univ.

Suzuki, A., & Kawahata, H. (2003). Carbon budget of coral reef systems: An overview of observations in fringing reefs, barrier reefs and atolls in the Indo-Pacific regions. *Tellus B*, *55*(2), 428–444. https://doi.org/10.1034/j.1600-0889.2003.01442.x

Teneva, L., Dunbar, R. B., Mucciarone, D. A., Dunckley, J. F., & Koseff, J. R. (2013). High-resolution carbon budgets on a Palau back-reef modulated by interactions between hydrodynamics and reef metabolism. *Limnology and Oceanography*, *58*(5), 1851–1870. https://doi.org/10.4319/lo.2013.58.5.1851

van Woesik, R., Houk, P., Isechal, J. W., Idechong, J. W., Victor, S., & Golbuu, Y. (2012). Climate-change refugia in the sheltered bays of Palau: Analogs of future reefs. *Ecology and Evolution*, *2*(10), 2474–2484. https://doi.org/10.1002/ece3.363

Watanabe, A. (2004). Process of seawater CO_2 system formation and biological community metabolism in coral reefs and brackish estuaries. Ph. D. thesis Univ. Tokyo.

Watanabe, A., Kayanne, H., Hata, H., Kudo, S., Nozaki, K., Katao, K., et al. (2006). Analysis of the seawater CO_2 system in the barrier reef—Lagoon system of Palau using total alkalinity-dissolved inorganic carbon diagrams. *Limnology and Oceanography*, *51*(4), 1614–1628. https://doi.org/10.4319/lo.2006.51.4.1614